Published in final edited form as:
J Proteome Res. 2012 December 7; 11(12): 5843–5855. doi:10.1021/pr3006167.

Proteome Analysis of Cry4Ba Toxin-Interacting *Aedes aegypti* Lipid Rafts using geLC-MS/MS

Krishnareddy Bayyareddy[a], **Xiang Zhu**[¶], **Ron Orlando**[¶], and **Michael J. Adang**[a,b,*]

[a]Department of Entomology, University of Georgia, Athens, GA, 30602, USA

[b]Department of Biochemistry and Molecular Biology, University of Georgia, Athens, GA, 30602, USA

[¶]Department of Complex Carbohydrate Research Center, University of Georgia, Athens, GA, 30602, USA

Abstract

Lipid rafts are microdomains in the plasma membrane of eukaryotic cells. Among their many functions, lipid rafts are involved in cell toxicity caused by pore forming bacterial toxins including *Bacillus thuringiensis* (Bt) Cry toxins. We isolated lipid rafts from brush border membrane vesicles (BBMV) of *Aedes aegypti* larvae as a detergent resistant membrane (DRM) fraction on density gradients. Cholesterol, aminopeptidase (APN), alkaline phosphatase (ALP) and the raft marker flotillin were preferentially partitioned into the lipid raft fraction. When mosquitocidal Cry4Ba toxin was pre-incubated with BBMV, Cry4Ba localized to lipid rafts. A proteomic approach based on one dimensional gel electrophoresis, in-gel trypsin digestion, followed by liquid chromatography-mass spectrometry (geLC-MS/MS) identified a total of 386 proteins. Of which many are typical lipid raft marker proteins including flotillins and glycosylphosphatidylinositol (GPI)-anchored proteins. Identified raft proteins were annotated *in silico* for functional and physicochemical characteristics. Parameters such as distribution of isoelectric point, molecular mass, and predicted post-translational modifications relevant to lipid raft proteins (GPI anchorage and myristoylation or palmitoylation) were analyzed for identified proteins in the DRM fraction. From a functional point of view, this study identified proteins implicated in Cry toxin interactions as well as membrane-associated proteins expressed in the mosquito midgut that have potential relevance to mosquito biology and vector management.

Keywords

Lipid rafts; Detergent resistant membranes; Brush border membrane vesicles; Cry4Ba toxin; Cholesterol; Proteomics; LC-MS/MS

INTRODUCTION

Lipid rafts are membrane micro-domains enriched in glycosylphosphatidylinositol (GPI)-anchored proteins, glycosphingolipids and sterols, and are defined by their insolubility in Triton X-100 at low temperature[1, 2]. In the literature lipid rafts have been frequently termed detergent-resistant membranes (DRMs) on the basis of detergent insolubility[3]. Lipid rafts

*Corresponding author. Michael J. Adang Department of Entomology, University of Georgia Phone: 706-542-2436. Fax: 706-542-2279. adang@uga.edu..

The authors have declared no conflict of interest.

Supporting Information Available: This material is available free of charge via the Internet at http://pubs.acs.org.

have been implicated in physiologically important cell membrane related processes including organizing and segregating membrane components for signaling, trafficking of plasma membrane proteins[4], and portals of entry for various pathogens, including viruses, bacteria and their toxins[5].

Bacterial pore forming toxins interact with host membrane receptors located in lipid rafts and this is a critical step in the oligomerization and insertion of these toxins into the membrane[6]. In some mammalian pore-forming bacterial toxins, lipid rafts play an essential role in toxin interaction by functioning as platforms to recruit distinct classes of proteins, such as GPI-anchored proteins and palmitoylated or diacylated transmembrane proteins[7]. Moreover, aerolysin, one of the most studied pore-forming toxins, functions via GPI-anchored proteins present in lipid rafts[8]. In insects, investigations regarding the presence of such microdomains and their interaction with insecticidal pore forming toxins are limited to a small number of recent studies. The presence and proper integrity of lipid rafts has been proposed as a prerequisite for Cry1A pore formation and toxicity, and also Cry1A receptor APN is localized to lipid raft domains of the plasma membrane in epithelial cells of *Heliothis virescens* and *Manduca sexta* larval midgut[9]. Bravo et al., reported cadherin, located outside of lipid rafts as binding Cry1Ab toxin inducing formation of an oligomeric toxin complex which then binds to APN driving the toxin oligomer into lipid raft microdomains causing pore formation[10]. Similarly, Cry1Ca was toxic to Sf9 cells after binding to lipid rafts, and without lipid rafts Sf9 cells showed resistance to Cry1Ca toxicity[11]. Toxin-mediated pores in the brush border membrane lead to osmotic cell shock, and finally cell death. Bt Cry protein mode-of-action and the usage of Bt were recently reviewed[12].

The yellow fever mosquito, *Aedes aegypti* is the major vector of dengue, yellow fever, and chikungunya viruses and represents a significant public health problem[13]. The most commonly used biolarvicide to control this vector is based on *Bacillus thuringiensis var. israelensis* (Bti). Bti harbors a megaplasmid which encodes multiple toxins: Cry4Aa, Cry4Ba, Cry10Aa, Cry11Aa, Cyt1Aa and Cyt-Ba[14]. Among these toxins Cry4Ba is more toxic to *A. aegypti* relative to the other individual toxins[15]. Cry4Ba and Cry11Aa toxins of Bti bind to specific receptor proteins on *Aedes* larval midgut cell surfaces and receptor binding has been shown to correlate with larval toxicity. These receptors[16] are cadherin[17], GPI- anchored ALPs[18–20] and GPI-anchored APNs[21, 22]. Some of these same receptor alkaline phosphatases and aminopeptidases have altered levels in an *Ae. aegypti* strain selected for Bti resistance[23].

Mass spectrometry-based proteomic identification can result in unique protein profiles of the lipid raft microenvironment and insight into functional processes of pathogen interactions. In non-insect systems several groups reported the protein composition of lipid rafts derived from brush border membranes[24–26]. These studies have indicated typical plasma membrane proteins such as GPI-ALPs, APNs, and other receptor proteins. In addition, signaling/ trafficking proteins belonging to the G protein family, protein kinases and the annexins were also identified. The brush border DRM proteome of adult *Anopheles gambiae* was recently reported[27]. The rationale for the *Anopheles* study was based on the probable DRM localization of attachment sites for the malarial parasite *Plasmodium* in midgut of adult *Anopheles*. Parish et al.[27] identified 1452 proteins including markers of DRMs including five *Plasmodium* ookinete binding proteins and 65 GPI-anchored proteins. The above cited studies have also shown that the global proteome composition of raft microdomains differs from that of the whole brush border membrane.

Here, we provide evidence for typical lipid raft characteristics in DRMs prepared from *A. aegypti* midgut membranes and demonstrate the interaction of Cry4Ba toxin with lipid rafts.

We also report the comprehensive proteome of the raft DRM fraction from mosquito larval BBMV. The geLC-MS/MS analysis of the DRM proteome identified a substantial number of high molecular weight and low abundance membrane bound proteins, including the known GPI-anchored APNs and ALPs that function as Cry4Ba receptors. These results will guide functional investigations of lipid rafts as a focal point for Bt Cry toxin action in mosquitoes.

EXPERIMENTAL PROCEDURES

Preparation of A. aegypti whole larval BBMV

A. aegypti (UGAL strain) was maintained as described[28]. Four grams early fourth instar larvae (stored −80°C) were suspended in 16 ml ice cold MET buffer (300 mM mannitol, 5 mM EGTA, 17 mM Tris-HCl, pH 7.5) containing 1 mM PMSF. Larvae were homogenized with 40 strokes of a teflon-glass homogenizer (clearance 0.1–0.15 mm; Wheaton) while rotating the pestle at 1525 rpm (GCA Precision Scientific). BBMV were prepared from the larval homogenate using the magnesium chloride precipitation method[29] with modifications[28]. The final BBMV pellet was suspended in 1 ml cold MET with Complete™ protease inhibitor cocktail (Roche Applied Science). Total protein concentrations were determined using a Bio-Rad protein assay kit (Bio-Rad) with bovine serum albumin as a protein standard (Sigma). The relative purity of the final BBMV preparation was assessed by comparing APN and ALP activities relative to the initial homogenate. APN and ALP activities of BBMV and extracted BBMV fractions (below) were determined using leucine-ρ-nitroanalide and ρ-nitrophenyl phosphate as substrates, respectively[30].

Extraction of a detergent resistant membrane fraction from A. aegypti larval BBMV and isolation on Optiprep™ density gradients

Detergent resistant membrane fractions (DRM) were prepared from larval BBMV using cold Triton X-100 extraction and Optiprep™ (Sigma) gradients[31]. BBMV (1mg) were re-suspended in 0.5 ml TNE buffer (25 mM Tris-HCl (pH 8.0), 150 mM NaCl, 5 mM EDTA), 0.5 ml ice-cold 2% Triton X-100 in TNE buffer was added, the mixture was gently suspended and placed on ice for 30 min. Extracted membrane solution was pipetted into a centrifuge tube and brought to 40% Optiprep™ by the addition of 2 ml 60% Optiprep™ in TNE buffer and then overlaid with 6 ml of 30% and 3 ml of 5% Optiprep™. Gradient were centrifuged (270519× g) in a SW41Ti (Beckman) rotor for 4 h at 4°C. After centrifugation, the opalescent DRM band was located at the interface between the 30% and 5% Optiprep™ gradients. Gradients fractions were collected from 12 one ml fractions starting from the top of the gradient.

Cholesterol quantitation and depletion from BBMV by methyl-β-cyclodextrin (MBCD)

Concentrations of cholesterol and cholesterol esters from the gradient fractions were determined in 96-well flat-well plates by Amplex® Red cholesterol assay kit (Invitrogen) according to the manufacturer's instruction. Briefly, 5 μl of each gradient fraction was mixed with 45 μl of 1× reaction buffer. A standard curve was made with cholesterol concentrations ranging from 1.25 μM to 12 μM with buffer as a negative control and 10 μM H_2O_2 as a positive control. Reactions were initiated by adding 50 μl Amplex® Red reagent/HRP/cholesterol oxidase/cholesterol esterase working solution to each well. Microplates were incubated for 30 min at 37°C in the dark. Reaction fluorescence was measured in BioTek Synergy 4 plate reader at an excitation wavelength of 550 nm and an emission wavelength of 590 nm over 30 min (5 min time points). Background fluorescence from the negative control reaction was subtracted from each value and determined unknown samples cholesterol concentration by comparing with a standard curve. For cholesterol depletion

experiments, BBMV were treated with 20 mM MBCD (Sigma) at 37°C for 60 min prior to detergent extraction and Optiprep™ fractionation.

Analysis of Cry4Ba toxin association with DRM extracted from BBMV

Cry4Ba association with DRM extracted from BBMV was analyzed as for Cry1Ab toxin-DRM interactions[9, 10]. Trypsin-activated Cry4Ba toxin was prepared from *E. coli*-produced inclusions[32]. BBMV (1mg) were incubated with 5 μg/ml Cry4Ba toxin in TNE buffer at 4°C overnight, subsequently the suspension was centrifuged 20442× g for 20 min and the pellet washed with TNE buffer twice. The washed BBMV pellet was treated with cold Triton X-100 and separated in Optiprep™ gradients as above. The effect of MBCD treatment on Cry4Ba association with DRM was examined by pre-incubating BBMV with 5 μg/ml of Cry4Ba toxin followed by MBCD treatment and DRM isolation. Equal volumes of gradient fractions were separated by SDS-10% PAGE, electro- transferred overnight on to polyvinylidene difluoride (PVDF) membrane, which were then identified by western blot analysis with anti-Cry4Ba serum as described below.

SDS-PAGE and Western Blotting

Equal sample volumes from the resulting gradient fractions were solubilized in 2× Laemmli buffer[33] and resolved on SDS-10% PAGE. Separated proteins were visualized either by silver staining, Deep Purple (GE Healthcare), or immunodetection on western blots as follows. Proteins were transferred by electro-blotting onto a PVDF membrane (overnight, 22v and 4°C; Criterion blotter (Bio-Rad) in transfer buffer (25 mM Tris, 192 mM glycine, 10% methanol). The membranes were blocked by incubating in PBST (137 mM NaCl, 2.7 mM KCl, 4.3 mM Na_2HPO4, 1.4 mM KH_2PO_4, 0.1% Tween 20) containing 3% BSA, followed by incubation with primary antibody diluted in PBST containing 1% BSA for 1 h. After washing the membranes for 3× 10 min, and then incubated in a PBST (1%BSA) containing secondary antibody conjugated to horseradish peroxidase (Molecular Probes). Finally, membranes were washed 3 times for 10 min in PBST and then incubated for 5 min with ECL™ detection reagent (GE Healthcare) and exposed to X-ray film to detect immunoreactive bands. All the incubations were at room temperature.

Preparation of in-gel protein digests

Biological replicates were prepared and analyzed as follows. Purified *A. aegypti* lipid raft proteins (20 μg) were resolved by SDS-10% PAGE and the gels stained with Deep Purple™ total protein stain according to the manufacturer's instructions (GE Healthcare). An individual gel lane was sliced into 20 pieces manually, and each piece was then subjected to dithiothreitol reduction, iodoacetamide alkylation, and in-gel trypsin digestion, using a standard protocol as previously reported[28]. The resulting tryptic peptides were extracted and concentrated to 20 μl each using a SpeedVac (Thermo Savant), and subjected to LC–MS/MS analysis.

LC-MS/MS analysis

Proteomic data was acquired using an Agilent 1100 Capillary LC system (Palo Alto, CA), using a 0.2 × 150 mm Halo Peptide ES-C18 capillary column packed with 2.7 μm diameter superficially porous particles (Advanced Materials Technology, Inc., Wilmington, DE). On-line MS detection used the Thermo-Fisher LTQ ion trap (San Jose, CA) with a Michrom (Michrom Bioresources, Auburn, CA) captive spray interface. Proteomic sample analysis utilized the LTQ divert valve fitted with an EXP Stem Trap 2.6 μL cartridge packed with Halo Peptide ES-C18 2.7 μm diameter superficially porous particles (Optimize Technologies, Oregon City, OR). Gradient conditions increased mobile phase B concentration from 6.25% to 75% B over 90 minutes at a flow rate of 4 μL/min. Mobile

phase A consisted of 99.9% water, 0.1% formic acid and 10 mM ammonium formate. Mobile phase B contained 80% acetonitrile, 0.1% formic acid and 10 mM ammonium formate. The instrument was set to acquire MS/MS spectra on the nine most abundant precursor ions from each MS scan. Dynamic exclusion was enabled for 90 s. Generated raw tandem mass spectra were converted into the mzXML format and then into peak lists using ReAdW software followed by mzMXL2Other software[34]. The peak lists were then searched using Mascot 2.2 (Matrix Science).

Database searching, protein identification and GPI-anchorage prediction

A target database was created using the Diptera annotated sequences obtained from Drosophila melanogaster, Anopheles gambiae, A. aegypti and *Culex quinquefasciatus* protein databases in Flybase version FB2008_07 (www.flybase.org) and Vectorbase version VB-2012-06 (www.vectorbase.org). A decoy database (decoy) was then constructed by reversing the sequences in the normal database. Using these databases we excluded redundancies and contaminations in the search results. Searches were performed against the normal and decoy databases using the following parameters: fully tryptic enzymatic cleavage with two possible missed cleavages, peptide tolerance of 1000 ppm, fragment ion tolerance of 0.6 Da. Fixed modification was set as carbamidomethyl due to carboxyamidomethylation of cysteine residues (+57 Da) and variable modifications were chosen as oxidation of methionine residues (+16 Da) and deamidation of asparagine residues (+1 Da). Statistically significant proteins from both searches were determined at a ≤1% protein false discovery rate (FDR) using the ProValT algorithm[35], as implemented in ProteoIQ (BioInquire). After sequences were identified they were annotated for possible function using QuickGO (http://www.ebi.ac.uk/QuickGO/Dataset.html). The big-PI predictor server (http://mendel.imp.ac.at/sat/gpi/gpi_server.html), GPI-SOM (http://gpi.unibe.ch/), and PredGPI (http://gpcr.biocomp.unibo.it/predgpi/pred.htm) were used to predict GPI anchorage of proteins. The computational tool CSS-Palm 3.0 (http://csspalm.biocuckoo.org/) was used to predict palmitoylation sites on proteins.

RESULTS

Cholesterol, flotillin, and the GPI-anchored proteins ALP and APN are concentrated in lipid rafts isolated from Aedes larval brush border membrane

Lipid rafts are defined by their insolubility in cold Triton X-100 and their density which helps them float on gradient solution. We used Optiprep™ gradient fractionation of 1% Triton X-100 solubilized BBMV. The lipid raft fraction was visible as an opalescent band at the 5%–30% interface (data not shown). Since cholesterol is typically enriched in DRM fractions (i.e. lipid rafts), we measured cholesterol content in the 12 collected gradient fractions. As shown in Fig. 1A, cholesterol content was highest in fraction 4 at the 5%–30% Optiprep™ interface. Fraction 4 contained about 50% of the total cholesterol present in all 12 fractions. In contrast, the majority (>50%) of the total protein was distributed in fractions 10–12 from the 40% Optiprep™ region; about 25% of total protein was in the DRM fraction 4. The enrichment of cholesterol versus total protein in the opalescent DRM fraction is consistent with a successful Optiprep™ gradient fractionation procedure for the isolation of *A. aegypti* lipid rafts.

Since GPI-anchored proteins are localized in DRM preparations, we measured the activities of ALP and APN across the Optiprep™ gradient. The enzymatic activities of ALP and APN were the highest in DRM fraction 4 with substantial APN activity spread across soluble fractions 4–9 (Fig. 1B). ALP activity was low in fractions 4–9 collected from the 30% Optiprep™ region but increased in the fractions 10–12 from the 40% Optiprep™ region. The result of probing a western blot of Optiprep™ fractions with anti-AgAPN1 antiserum is

shown in Fig. 2C. AgAPN1 (AGAP004809) is a midgut brush border APN identifed in *An. gambiae* adults and anti-AgAPN1 serum inhibits development of the malarial parasite in mosquitoes[36]. AgAPN1 has 60% protein identity with APN1 (AAEL012778) the Cry4Ba, Cry11Aa and Cry11Ba receptor in *A. aegypti*[16, 21, 22]. The distribution of APN protein detected by anti-serum was in agreement with the activity data. The strongest signal for APN was in DRM fraction 4, yet an APN signal was detectable in 30% Optiprep™ fractions 4–9. We probed blots of the Optiprep™ fractions with anti-AeFlot-1 antibody to determine the distribution of flotillin in the gradient. As shown in Fig. 2B, the flotillin amount was greatest in the DRM fraction 4, with lesser amounts in fractions 5–9, there was little flotillin detected in the soluble protein fractions 10–12. The highest concentration of flottilin, cholesterol, APN and ALP were each located in fraction 4, providing further support that fraction 4 from the Optiprep™ gradients is the lipid raft fraction.

Cry4Ba toxin is associated with the A. aegypti lipid rafts

Cry4Ba binds APNs and ALPs in *Aedes* midgut[16, 28], therefore we hypothesized that membrane-bound Cry4Ba would localize in the DRM fraction of *Aedes* brush border membranes. To test this hypothesis, BBMV were pre-incubated with Cry4Ba toxin. After unbound toxin was removed by washing BBMV and cold Triton X-100 extraction, soluble and insoluble materials were separated by flotation on Optiprep™ step gradients and the distribution of Cry4Ba toxin was analyzed by probing blots with anti-Cry4Ba antibody. As seen in Fig. 2D, most of the toxin was in the DRM fraction 4 with some toxin in soluble fractions 10–12. The association of Cry4Ba with the *A. aegypti* DRM fraction suggests that raft microdomains play a key role in membrane insertion and pore formation.

Effect of MBCD on A. aegypti lipid raft cholesterol and protein distribution

MBCD extracts cholesterol from lipid rafts causing a loss of integrity when raft integrity depends on cholesterol[37]. To test the effect of cholesterol depletion by MBCD on *Aedes* larval lipid rafts, BBMV were pre-incubated with MBCD, extracted with cold Triton-X100 and the extract separated by Optiprep™ gradient fractionation. Surprisingly, a fraction of the *Aedes* membrane was resistant to Triton X-100 and floated at the interface between 5% and 30% Optiprep™. Fraction 4, the floating fraction, showed the highest cholesterol and total protein content (Fig. 3A). Less than 10% of total protein was in the high-density soluble fractions. Following the MBCD treatment, the amounts of cholesterol and protein in raft fractions 4 and 5 were slightly higher than untreated BBMV (Fig. 3A). Thus, incubation of BBMV with MBCD under conditions that induce cholesterol depletion did not disrupt the DRM lipid raft fraction.

We also tested APN and ALP enzyme activities in the MBCD pre-treated gradient fractions and the results differed for the two enzymes. While APN activity was concentrated in the DRM fraction, ALP activity could no longer be detected in any gradient fractions (Fig. 3B). The ALP activity results suggest that under MBCD incubation conditions ALP may degraded or possibly MBCD interferes with the ALP reaction. The results of activity assays with BBMV and ALP substrate with or without MBCD showed no difference attributable to MBCD (data not shown).

Further evidence for the resistance of the DRM fraction to MBCD is presented in Fig. 3C showing where anti-AeFlot1 antibody detected a 47-kDa protein in fraction 4. Albeit, MBCD treatment did reduce the flotillin signal in fractions 5 –9 suggesting that MBCD was having some affect on BBMV materials in this Optiprep gradient fractions. Additionally, MBCD treatment did not affect localization of Cry4Ba to the DRM fraction (Fig. 3D).

In summary, the distribution pattern of cholesterol and marker protein activity assays and the western blots of flotillin-1, APN-1, and Cry4Ba, clearly evidenced co-partitioning of both Cry4Ba toxin and lipid raft marker proteins in the DRM lipid raft fractions. When MBCD was used on BBMV, DRM association of cholesterol, marker proteins and Cry4Ba were essentially unaffected. Furthermore, the data suggested a preferential association of Cry4Ba with lipid rafts in *A. aegypti*.

Proteomic analysis of lipid rafts isolated from A. aegypti BBMV

The member proteins of the DRM fraction were identified as diagrammed in Fig. 4. The opalescent band at the 5%–30% Optiprep™ interface was collected and the proteins separated by SDS-PAGE. After staining the gel, twenty equal gel sections were excised from and subjected to trypsin in-gel digestion. The resulting peptides in each gel sections were separated and analyzed by LC-MS/MS. The peptide sequences deduced from mass spectrometry were matched to *A. aegypti* proteins using the Mascot search engine against either the *A. aegypti* database alone, or the combined Diptera databases. For Mascot search results obtained against Diptera database, if two or more potential matches were reported for one mass spectrum, only peptide hits with the highest matching score (i.e., No.1 ranking) for the corresponding spectra were selected.

Our analysis revealed 1513 unique peptides representing 312 proteins in the first DRM sample and 2760 unique peptides representing 290 proteins in the second DRM sample set, all of which passed a <1% false discovery rate (Table S1). Of the 290 proteins, 208 were common to both biological replicates and the 50 GPI-anchored proteins identified in replicate 1 were present in replicate 2 plus acetylcholinesterase and an additional vanin-like protein 1. Of the 386 total proteins, 352 proteins were identified with two or more unique peptide sequences of which 4 proteins matched to conserved hypothetical proteins not assigned to any known protein in the constructed Diptera database. For these uncharacterized proteins, no homolog that satisfied BLAST criteria was found when their sequence was searched against NCBInr database. Using stringent statistical analysis via ProteoIQ, 34 proteins identified with a single peptide were accepted if the peptide occurred multiple times in the data set.

The distribution of predicted isolectric points (pI) and molecular masses of identified DRM proteins (Table S1) are presented in Fig. 5. The pI of the proteins identified range from 3.9 to 12.2 with a peak of proteins (about 40%) in the acidic pH 4–6 range; 2D gels of *Aedes* larval BBMV proteins have a similar concentration of proteins in the acidic range[28]. Of the total DRM proteins 54% have predicted pI values less than 7 and 46% greater than 7 (Fig. 5A). The molecular masses of the identified proteins ranged between 8 and 300 kDa with a majority of proteins (94%) exhibiting a molecular mass <120 kDa (Fig. 5B). Some of the identified proteins, such as apolipophorin II, are probably pro-proteins and do not represent final size of proteins expected to be present in the DRMs.

The identified proteins listed in Table S1 were also classified on the basis of their subcellular localization, molecular function and biological process as predicted from their gene ontology (GO) term descriptions provided in FlyBase and UniProtKB database. Apart from this, for each identified protein GO terms were compared with results from other studies. Functional classification of the all uniquely identified proteins is shown in Fig. 6. Of the 342 proteins identified with protein names, 293 had descriptions for their molecular function and these were summarized into 13 GO categories. These proteins are involved in: binding, (59 proteins); translation elongation (47 proteins); peptidase activity (44 proteins); cellular metabolic processes (49 proteins); cell transport (38 proteins); proteins with Unknown GO terms (49 proteins); hydrolase activity (14 proteins); transferase activity (9 proteins); cell signaling (9 proteins); phosphatase activity (8 proteins); isomerase activity (6

proteins); Receptors or surface glycoproteins functions (6 proteins), and oxidoreductase activity (4 proteins); see Fig. 6B for assignments for individual proteins.

When we analyzed the identified 342 proteins for subcellular locations, 96 proteins did not have descriptions for GO terms. A large proportion of the identified proteins are known or were predicted to be associated with plasma membranes, with 26% described as membrane-bound, 3% integral to membrane, and 2% are associated extracellular. For the remainder of the proteins, 14% are localized in cytoplasm, 13% in lipid particles, and 9% are associated with mitochondria. Proteins involved in the cytoskeleton accounted for 6%; 28% of the identified proteins did not have GO terms defined (Fig. 6A).

The results of GO analysis for the 342 annotated proteins identified into known biological processes are shown in Fig. 6C. The most numerously identified proteins belong to the following categories: Metabolism and biogenesis (38%), biological regulation (25%), ion transport (8%), immune system process (9%), cytoskeletal component organization (5%) and cell biological process unknown (16%).

DISCUSSION

The brush border membrane of *Aedes* larvae has a lateral organization that includes a DRM fraction containing lipid rafts. The DRM fraction was prepared from *Aedes* larval BBMV using cold Triton X-100 extraction and Optiprep™ gradient fractionation. The DRM fraction was enriched in cholesterol, and alkaline phosphatase and aminopeptidase activities (Fig. 1). Western blot analysis identified AeFlot-1 and APN1 in the DRM fraction (Fig. 2B and 2C). These results and the proteomic analyses of the DRMs identified GPI-anchored proteins and other lipid-raft associated proteins, a result in agreement with studies conducted on vertebrate systems[24, 26, 38, 39].

Cry4Ba toxin association with A .aegypti lipid rafts

The presence of lipid rafts in the DRM fraction provided an approach to bridge the model that Cry1 toxins insert into lipid rafts[9–11] to mosquitocidal Cry toxins. The detection of membrane-bound Cry4Ba toxin in the DRM fraction (Fig. 2D) is in concordance with the Cry1 insertion model and in agreement with the presence of Cry4Ba receptor APNs[22] and ALP[19] in the raft fraction (Fig. 2C, 1B and Table S1). Possibly the small amount of bound Cry4Ba in the soluble membrane fraction (Fig. 2D) may be attributed to non-specific Cry4Ba binding to BBMV or binding to receptors that are not raft-associated. The integration of Cry4Ba into the lipid raft component of the DRMs supports the model that lipid rafts have a functional role in the Cry intoxication process in mosquito larvae, as they do for Cry toxin action in lepidopteran larvae.

Effect of MBCD on Cry 4Ba and receptors distribution

The integrity of DRM fractions in plasma membranes typically depends on cholesterol and sphingolipids[40, 41]. Consequently, extraction of cholesterol with MBCD often disrupts the DRM and releases associated proteins into the soluble phase of a sucrose or Optiprep™ gradient[42, 43]. We tested the influence of MBCD on the brush border DRM fraction by treating BBMV with MBCD prior to Triton X-100 extraction and Optiprep ™gradient fractionation. After MBCD treatment, we observed no obvious physical change in the opalescent DRM band and detected no changes in cholesterol, APN or flotillin and no loss of the ability of Cry4Ba to partition into the DRM fraction (Fig. 3). What may account for the stability of the *Aedes* DRM fraction after extraction of BBMV with MBCD? It is possible that the low concentration of cholesterol in mosquito midgut membrane may limit the ability of MBCD to effectively bind and extract cholesterol. MBCD depletion of

cholesterol from membranes is limited or slower in membranes with low cholesterol content[44, 45] and high sphingomyelin content[46]. It is also possible that while MBCD selectively extracts cholesterol, *A. aegypti* larvae may have other sterols or membrane components involved in maintaining raft integrity resulting in a cholesterol-independent DRM fraction. For example, similar to mammalian brush rafts membranes insect brush border membranes contain glycosphingolipids[2] and galectin (Table S1). In mammalian brush border membranes, galectin stabilizes lipid rafts by cross-linking glycosophingolids resulting in cholesterol-independent rafts[47, 48]. With respect to Cry4Ba partitioning into DRMs after MBCD treatment of BBMV (Fig. 3D), this is consistent with MBCD-resistance of the DRMs. Additionally, previous studies with other pore forming toxins in mammalian cells indicated that the MBCD had no effect on toxin association and gradient distribution[49, 50].

Proteomic profile of the DRM fraction from Aedes larval midgut brush border membranes

Proteomic analyses of insect midguts have characterized either total BBMV proteomes[51, 52] or a proteome subset such as Bt toxin binding proteins[28, 53, 54]. Our geLC-MS/MS analysis of the DRM sub-proteome identified lipid raft marker proteins flotillin-1, flotillin-2, APN and ALP and many other proteins reported in similar analyses of DRMs[55–59]. The 386 identified proteins (342 annotated proteins) are just slightly less in number than the approximately 400 spots seen on a 2D gel of *Aedes* brush border proteins[28, 51]. In comparison, microarray experiments identified 3512 transcripts in midgut of *Ae. aegypti* larvae[23]. Of the 342 annotated proteins (Table S1) an expected overlap in identified DRM proteins was observed with the published *Aedes* larval BBMV proteome study[51]. Those authors identified 89 abundant proteins by a combination of 2D gel and LC-MS/MS approaches and of these 22 were identified in our DRM fraction. In addition to identifying about 290 proteins not detected in *Aedes* larval BBMV[51], our DRM proteomic analysis identified more members of each type of GPI-anchored protein family (6 alkaline phosphatases, 10 m1 class aminopeptidases, and 5 alpha-amylases and 2 carbonic anhydrases) versus the single member identified in the *Aedes* BBMV larval proteome. Flotillins were identified in our DRM fraction and in our proteomics-based search for Cry4Ba binding proteins in *Aedes* BBMV, but not in Popova-Butler Dean's study[51].

GPI-anchored proteins are targeted to lipid rafts and enriched in DRMs[2, 38]. Consistent with the localization of GPI-anchored proteins in DRMS, bioinformatic analyses of *Aedes* DRM proteins predicts 64 proteins as having GPI-anchors (Table 1). Each of the 4 GPI predictor programs identified a set of proteins including alanyl aminopeptidase, alkaline phosphatase, alpha-amylase, an m1 metalloprotease (APN), and carbonic anhydrase as likely to have a GPI-anchor. ALP and APN proteins were previously confirmed as GPI-anchored proteins and identified as receptors for Cry toxins in *Aedes* mosquito larvae. See Table 2 for a listing of ALPs and APNs identified as Bti Cry binding proteins and receptors. For example, ALPs are identified as Cry4Ba binding and possible receptor proteins and ALP AAEL015070 in group 7 according to[16], was recently identified as a functional Cry4Ba receptor[19] (Table 2). However, AeALP1 (AAEL009077) , which is a receptor of Cry11Aa and Cry4Ba in *Aedes* larvae[18, 20], was not detected in DRMs in either replicate 1 or 2. Two ALPs (AAEL003313 & AAEL003298) identified in DRMs were recently shown to be down-regulated in a Bti resistant *A. aegypti* strain[23]. Aminopeptidase AEL01278 (named AeAPN1) was identified as a receptor for Cry4Ba and Cry11Aa and in *Aedes* larvae[21, 22] (Table 2). This is the only GPI-anchored APN identified by each of the 4 GPI predictor programs. Two APNs (AAEL008155; called AeAPN2) and AAEL012774 (AeAPN4) were identified in *Aedes* BBMV as binding Cry11Aa[16]. Also, one APN (AAEL012774) was up-regulated and another APN down-regulated (AAEL012776) in the Bti resistant *A. aegypti* strain[23]. However, according to analyses of the annotated APNs they are not predicted to have GPI

anchors (Table 1). Incorrect annotation of the APNs in the *Aedes* database is a possible explanation for lack of a predicted GPI anchor. Alternatively, these APNs are attached to brush border membrane via another anchorage system (discussed below). In regards to the glucosidase with predicted GPI anchorage, interestingly, the glucosidase present in DRM is not the GPI-anchored glucosidase which was examined, but refuted, as a receptor to mosquitocidal Bin toxin[60]. Overall, most of the predicted GPI-anchored proteins present in *Aedes* DRM are glycosidases and hydrolases. Other notable proteins in the DRM fraction with predicted GPI-anchorage include carbonic anhydrase, an enzyme involved in alkalinization of *Aedes* midgut[61]. Lachesin, a protein involved in epithelial integrity[62] was detected and probably identified correctly as a GPI-anchored protein. An apyrase and apolipoprotein D also had signals for GPI-anchorage recognized by each software program.

Predicted S-acylated proteins in the DRM fraction

Some proteins are targeted and attached to membranes via a post-translationally attached fatty acid. The most common type of attachment is via S-acylation at cysteine residues where the attached moiety is palmitic acid, hence the common name palmitoylation[63]. Palmitoylated proteins are frequently isolated in DRMs and are considered lipid rafts components[64]. Using the computer program CSS-Palm[65], the set of identified DRM proteins was searched for predicted palmitoylation sites yielding a list of 222 proteins (Table S2). The caveat with this analysis is that because of a lack of experimental validation it is unclear how well the predictions correlate with actual palmitoylation. Several cytoskeletal proteins, including actin, myosin and tubulin, were identified as having putative palmitoylation sites and in cultured human cells their homologues are palmitoylated and raft-associated[64]. This assemblage of cytoskeletal proteins in the DRM fraction also correlates with the link between lipid rafts, cytoskeletal proteins intracellular structures[64]. Several 40s and 60S ribosomal proteins have predicted palmitoylation sites and they also have counterparts in human cells[64]. The CSS-Palm program also identified a number of ALPs and APNs as having palmitoylation sites. If APNs are indeed attached to brush border membrane via palmitoylation, it would explain why in insect BBMV preparations only half of the APN activity is released by the phosphatidylinositolspecific phospholipase C which cleaves GPI-anchored proteins[66]. Overall, there is correlation between proteins having predicted palmitoylation sites and their protein localization according to GO annotation.

Proteins not expected to be in lipid rafts that are likely contaminants of the DRM

The presence of ribosomal, mitochondrial, and endoplasmic reticulum proteins in the DRM fraction is consistent with the DRM literature[55, 58, 67, 68]. As discussed above some of the proteins typically with these organelles may be present in DRMs because they are lipidated (i.e palmitoylated). Another explanation is that these subcellular organelles are entrapped in BBMV during the folding process that occurs during the process of gut homogenization and vesicle purification[69, 70]. In the case of mitochondria, they do not have lipid rafts and are considered contaminants in DRM preparations[71]. This conclusion was based on proteomic analyses of DRMs and mitochondria from cultured human cells where F1/F0 ATPase subunits and other mitochondrial proteins were identified as co-purifying contaminants in DRM/lipid raft preparations[71]. With respect to BBMV[51] and the DRM fraction analyzed in this study, it is possible that extra purification steps in BBMV and further development of the step gradient technique could yield improved BBMV and DRM fractions. However, it is likely that small contamination will always show up in the proteomes of insect BBMV and lipid rafts, since LC-MS/MS is such an ultra-sensitive technique. Therefore, it is very important to re-evaluate the DRM fractions using qualitative immunoblotting and immunolocalization techniques. New techniques based on in vivo labeling and quantitative mass spectrometries are likely to add insights into DRM composition and their included lipid rafts. Based on these observations, the existence of rafts in cell organelles, BBMV

preparation, and co-precipitation of cell organelle proteins with lipid rafts deserves serious consideration.

CONCLUSION

We believe that our observations, together with the information available for Bt toxins in other insects, also demonstrated the existence of lipid rafts in insects and their interaction with Bt Cry pore forming toxins.

In recent years, our knowledge of the Bt toxin receptors on the membrane surface and their complex interaction has improved significantly. Even though most of the knowledge of Bt toxin receptors and toxin mode of action is derived from lepidopteran studies, there are broad differences in the midgut physiology of lepidopterans and dipteran insects. Although many receptors for of the Bt toxin are still unknown, many toxins seem to have an affinity for the same class of proteins on the midgut cells. Proteome composition of lipid rafts, which is an important target site for both mosquito killing and vectored pathogens helps in designing better mosquito control strategies. Several studies have suggested many pathogens interact with lipid rafts. However, specific interacting proteins have not yet been identified; our study should help in the characterization and also in identifying candidate proteins that control susceptibility to Bt toxins. In this relatively new field, more research is needed to knock down the function of key lipid raft proteins. It will have better clarity on developing effective management strategies directed at vector controlling and also preventing toxin resistance in the mosquitoes. Furthermore, it may also serve as an important early step toward limiting the spread and burden of human disease caused by pathogens that are vectored by mosquitoes in general and *A. aegypti* in particular.

Supplementary Material

Refer to Web version on PubMed Central for supplementary material.

Acknowledgments

This research was partially supported by National Institutes of Health Grant R01 AI 29092 to D.H. Dean (Ohio State University) and M.J.A. The authors acknowledge Dr. Rhoel D.R. Dinglasan (Johns Hopkins University) for providing anti-AgAPN1 serum. The authors thank Dr. Mohd Amir F. Abdullah for fruitful discussions and Darryl Johnson (UGA, CCRC) for assistance with LC-MS/MS analysis of the second biological replicate.

ABBREVIATIONS

ALP	alkaline phosphatase
APN	aminopeptidase
Bti	Bacillus thuringiensis israelensis
BBMV	brush border membrane vesicles
DRM	detergent resistant membranes
geLC-MS/MS	gel electrophoresis liquid chromatrography-mass spectrometry/mass spectrometry
GPI	glycosyl phosphatidyl inositol
MBCD	methyl-B-cyclodextrin

REFERENCES

(1). Lingwood D, Simons K. Lipid rafts as a membrane-organizing principle. Science. 2010; 327(5961):46–50. [PubMed: 20044567]

(2). Rietveld A, Neutz S, Simons K, Eaton S. Association of sterol- and glycosylphosphatidylinositol-linked proteins with *Drosophila* raft lipid microdomains. J Biol Chem. 1999; 274(17):12049–12054. [PubMed: 10207028]

(3). Brown DA. Lipid rafts, detergent-resistant membranes, and raft targeting signals. Physiology (Bethesda). 2006; 21:430–439. [PubMed: 17119156]

(4). Schroeder RJ, Ahmed SN, Zhu Y, London E, Brown DA. Cholesterol and sphingolipid enhance the Triton X-100 insolubility of glycosylphosphatidylinositol-anchored proteins by promoting the formation of detergent-insoluble ordered membrane domains. J Biol Chem. 1998; 273(2):1150–1157. [PubMed: 9422781]

(5). Fantini J, Garmy N, Mahfoud R, Yahi N. Lipid rafts: structure, function and role in HIV, Alzheimer's and prion diseases. Expert Rev Mol Med. 2002; 4(27):1–22. [PubMed: 14987385]

(6). Cabiaux V, Wolff C, Ruysschaert J-M. Interaction with a lipid membrane: a key step in bacterial toxins virulence. Int J Biol Macromol. 1997; 21(4):285–298. [PubMed: 9493052]

(7). Galbiati F, Razani B, Lisanti MP. Emerging themes in lipid rafts and caveolae. Cell. 2001; 106(4): 403–411. [PubMed: 11525727]

(8). Abrami L, Fivaz M, Decroly E, Seidah NG, Jean F, Thomas G, Leppla SH, Buckley JT, van der Goot FG. The pore-forming toxin proaerolysin is activated by furin. J Biol Chem. 1998; 273(49): 32656–32661. [PubMed: 9830006]

(9). Zhuang M, Oltean DI, Gomez I, Pullikuth AK, Soberon M, Bravo A, Gill SS. *Heliothis virescens* and *Manduca sexta* lipid rafts are involved in Cry1A toxin binding to the midgut epithelium and subsequent pore formation. J Biol Chem. 2002; 277(16):13863–13872. [PubMed: 11836242]

(10). Bravo A, Gómez I, Conde J, Muñoz-Garay C, Sánchez J, Miranda R, Zhuang M, Gill SS, Soberón M. Oligomerization triggers binding of a *Bacillus thuringiensis* Cry1Ab pore-forming toxin to aminopeptidase N receptor leading to insertion into membrane microdomains. Biochim Biophys Acta. 2004; 1667(1):38–46. [PubMed: 15533304]

(11). Avisar D, Segal M, Sneh B, Zilberstein A. Cell-cycle-dependent resistance to *Bacillus thuringiensis* Cry1C toxin in Sf9 cells. J Cell Sci. 2005; 118(Pt 14):3163–3171. [PubMed: 15985466]

(12). Bravo A, Likitvivatanavong S, Gill SS, Soberon M. *Bacillus thuringiensis*: A story of a successful bioinsecticide. Insect Biochem Mol Biol. 2011; 41(7):423–431. [PubMed: 21376122]

(13). Chadee DD, Kittayapong P, Morrison AC, Tabachnick WJ. A breakthrough for global public health. Science. 2007; 316(5832):1703–1704. [PubMed: 17588917]

(14). Berry C, O'Neil S, Ben-Dov E, Jones AF, Murphy L, Quail MA, Holden MT, Harris D, Zaritsky A, Parkhill J. Complete sequence and organization of pBtoxis, the toxin-coding plasmid of *Bacillus thuringiensis* subsp. *israelensis*. Appl Environ Microbiol. 2002; 68(10):5082–5095. [PubMed: 12324359]

(15). Poncet S, Delécluse A, Klier A, Rapoport G. Evaluation of synergistic interactions among the CryIVA, CryIVB, and CryIVD toxic components of *B. thuringiensis* subsp. *israelensis* crystals. J Invertebr Pathol. 1995; 66(2):131–135.

(16). Likitvivatanavong S, Chen J, Evans AM, Bravo A, Soberon M, Gill SS. Multiple receptors as targets of Cry toxins in mosquitoes. J Agric Food Chem. 2011; 59(7):2829–2838. [PubMed: 21210704]

(17). Chen J, Aimanova KG, Fernandez LE, Bravo A, Soberon M, Gill SS. *Aedes aegypti* cadherin serves as a putative receptor of the Cry11Aa toxin from *Bacillus thuringiensis* subsp. *israelensis*. Biochem J. 2009; 424(2):191–200. [PubMed: 19732034]

(18). Fernandez LE, Aimanova KG, Gill SS, Bravo A, Soberon M. A GPI-anchored alkaline phosphatase is a functional midgut receptor of Cry11Aa toxin in *Aedes aegypti* larvae. Biochem J. 2006; 394(Pt 1):77–84. [PubMed: 16255715]

(19). Dechklar M, Tiewsiri K, Angsuthanasombat C, Pootanakit K. Functional expression in insect cells of glycosylphosphatidylinositol-linked alkaline phosphatase from *Aedes aegypti* larval

midgut: A *Bacillus thuringiensis* Cry4Ba toxin receptor. Insect Biochem Mol Biol. 2011; 41(3): 159–166. [PubMed: 21146607]

(20). Jimenez AI, Reyes EZ, Cancino-Rodezno A, Bedoya-Perez LP, Caballero-Flores GG, Muriel-Millan LF, Likitvivatanavong S, Gill SS, Bravo A, Soberon M. *Aedes aegypti* alkaline phosphatase ALP1 is a functional receptor of *Bacillus thuringiensis* Cry4Ba and Cry11Aa toxins. Insect Biochem Mol Biol. 2012

(21). Chen J, Aimanova KG, Pan S, Gill SS. Identification and characterization of *Aedes aegypti* aminopeptidase N as a putative receptor of *Bacillus thuringiensis* Cry11A toxin. Insect Biochem Mol Biol. 2009; 39(10):688–696. [PubMed: 19698787]

(22). Saengwiman S, Aroonkesorn A, Dedvisitsakul P, Sakdee S, Leetachewa S, Angsuthanasombat C, Pootanakit K. In vivo identification of *Bacillus thuringiensis* Cry4Ba toxin receptors by RNA interference knockdown of glycosylphosphatidylinositol-linked aminopeptidase N transcripts in *Aedes aegypti* larvae. Biochem Biophys Res Commun. 2011; 407(4):708–713. [PubMed: 21439264]

(23). Tetreau G, Bayyareddy K, Jones CM, Stalinski R, Riaz MA, Paris M, David JP, Adang MJ, Despres L. Larval midgut modifications associated with Bti resistance in the yellow fever mosquito using proteomic and transcriptomic approaches. BMC Genomics. 2012; 13:248. [PubMed: 22703117]

(24). Nguyen HTT, Amine AB, Lafitte D, Waheed AA, Nicoletti C, Villard C, Létisse M, Deyris V, Rozière M, Tchiakpe L, Danielle C-D, Comeau L, Hiol A. Proteomic characterization of lipid rafts markers from the rat intestinal brush border. Biochem Biophys Res Commun. 2006; 342(1): 236–244. [PubMed: 16480947]

(25). Paradela A, Bravo SB, Henríquez M, Riquelme G, Gavilanes F, González-Ros JM, Albar JP. Proteomic analysis of apical microvillous membranes of syncytiotrophoblast cells reveals a high degree of similarity with lipid rafts. J Proteome Res. 2005; 4(6):2435–2441. [PubMed: 16335998]

(26). Gylfason GA, Knutsdottir E, Asgeirsson B. Isolation and biochemical characterisation of lipid rafts from Atlantic cod (*Gadus morhua*) intestinal enterocytes. Comp Biochem Physiol, Part B: Biochem Mol Biol. 2010; 155(1):86–95.

(27). Parish LA, Colquhoun DR, Mohien CU, Lyashkov AE, Graham DR, Dinglasan RR. Ookinete-interacting proteins on the microvillar surface are partitioned into detergent resistant membranes of *Anopheles gambiae* midguts. J. of Proteome Res. 2011

(28). Bayyareddy K, Andacht TM, Abdullah MA, Adang MJ. Proteomic identification of *Bacillus thuringiensis* subsp. *israelensis* toxin Cry4Ba binding proteins in midgut membranes from *Aedes* (*Stegomyia*) *aegypti* Linnaeus (Diptera, Culicidae) larvae. Insect Biochem Mol Biol. 2009; 39(4): 279–286. [PubMed: 19272330]

(29). Silva-Filha MH, Nielsen-Leroux C, Charles J-F. Binding kinetics of *Bacillus sphaericus* binary toxin to midgut brush-border membranes of *Anopheles* and *Culex sp*. mosquito larvae. EurJBiochem. 1997; 247:754–761.

(30). Terra WR, Ferreira C. Insect digestive enzymes: properties, compartmentalization and function. Comp Biochem Physiol, Part B: Biochem Mol Biol. 1994; 109B:1–62.

(31). Chmelar RS, Nathanson NM. Identification of a novel apical sorting motif and mechanism of targeting of the M2 muscarinic acetylcholine receptor. J Biol Chem. 2006; 281(46):35381–35396. [PubMed: 16968700]

(32). Abdullah MA, Alzate O, Mohammad M, McNall RJ, Adang MJ, Dean DH. Introduction of *Culex* toxicity into *Bacillus thuringiensis* Cry4Ba by protein engineering. Appl Environ Microbiol. 2003; 69(9):5343–5353. [PubMed: 12957922]

(33). Laemmli UK. Cleavage of structural proteins during the assembly of the head of bacteriophage T4. Nature. 1970; 227:680–685. [PubMed: 5432063]

(34). Pedrioli PGA, Eng JK, Hubley R, Vogelzang M, Deutsch EW, Raught B, Pratt B, Nilsson E, Angeletti RH, Apweiler R, Cheung K, Costello CE, Hermjakob H, Huang S, Julian RK, Kapp E, McComb ME, Oliver SG, Omenn G, Paton NW, Simpson R, Smith R, Taylor CF, Zhu W, Aebersold R. A common open representation of mass spectrometry data and its application to proteomics research. Nat Biotech. 2004; 22(11):1459–1466.

(35). Weatherly DB, Atwood JA 3rd, Minning TA, Cavola C, Tarleton RL, Orlando R. A Heuristic method for assigning a false-discovery rate for protein identifications from Mascot database search results. Molecular & cellular proteomics : MCP. 2005; 4(6):762–772.

(36). Dinglasan RR, Kalume DE, Kanzok SM, Ghosh AK, Muratova O, Pandey A, Jacobs-Lorena M. Disruption of *Plasmodium falciparum* development by antibodies against a conserved mosquito midgut antigen. Proc Natl Acad Sci U S A. 2007; 104(33):13461–13466. [PubMed: 17673553]

(37). Schuck S, Honsho M, Ekroos K, Shevchenko A, Simons K. Resistance of cell membranes to different detergents. Proc Natl Acad Sci U S A. 2003; 100(10):5795–5800. [PubMed: 12721375]

(38). Brown DA, Rose JK. Sorting of GPI-anchored proteins to glycolipid-enriched membrane subdomains during transport to the apical cell surface. Cell. 1992; 68(3):533–544. [PubMed: 1531449]

(39). Danielsen EM. Involvement of detergent-insoluble complexes in the intracellular transport of intestinal brush border enzymes. Biochemistry. 1995; 34(5):1596–1605. [PubMed: 7849019]

(40). Brown DA, London E. Functions of lipid rafts in biological membranes. Annu Rev Cell Dev Biol. 1998; 14:111–136. [PubMed: 9891780]

(41). Simons K, Ikonen E. Functional rafts in cell membranes. Nature. 1997; 387(6633):569–572. [PubMed: 9177342]

(42). Crepaldi Domingues C, Ciana A, Buttafava A, Balduini C, de Paula E, Minetti G. Resistance of human erythrocyte membranes to Triton X-100 and C12E8. J Membr Biol. 2009; 227(1):39–48. [PubMed: 19067023]

(43). Kamata K, Manno S, Ozaki M, Takakuwa Y. Functional evidence for presence of lipid rafts in erythrocyte membranes: Gsα in rafts is essential for signal transduction. Am J Hematol. 2008; 83(5):371–375. [PubMed: 18181202]

(44). Besenicar MP, Bavdek A, Kladnik A, Macek P, Anderluh G. Kinetics of cholesterol extraction from lipid membranes by methyl-beta-cyclodextrin--a surface plasmon resonance approach. Biochim Biophys Acta. 2008; 1778(1):175–184. [PubMed: 18068686]

(45). Jouni ZE, Zamora J, Wells MA. Absorption and tissue distribution of cholesterol in *Manduca sexta*. Arch Insect Biochem Physiol. 2002; 49(3):167–175. [PubMed: 11857677]

(46). Sano O, Kobayashi A, Nagao K, Kumagai K, Kioka N, Hanada K, Ueda K, Matsuo M. Sphingomyelin-dependence of cholesterol efflux mediated by ABCG1. J Lipid Res. 2007; 48(11):2377–2384. [PubMed: 17761632]

(47). Braccia A, Villani M, Immerdal L, Niels-Christiansen L-L, Nystrøm BT, Hansen GH, Danielsen EM. Microvillar membrane microdomains exist at physiological temperature. J Biol Chem. 2003; 278(18):15679–15684. [PubMed: 12594212]

(48). Hansen GH, Immerdal L, Thorsen E, Niels-Christiansen L-L, Nystrøm BT, Demant EJF, Danielsen EM. Lipid rafts exist as stable cholesterol-independent microdomains in the brush border membrane of enterocytes. J Biol Chem. 2001; 276(34):32338–32344. [PubMed: 11389144]

(49). Hansen GH, Dalskov S-M, Rasmussen CR, Immerdal L, Niels-Christiansen L-L, Danielsen EM. Cholera toxin entry into pig enterocytes occurs via a lipid raft- and clathrin-dependent mechanism. Biochemistry. 2004; 44(3):873–882. [PubMed: 15654743]

(50). Shogomori H, Futerman AH. Cholera toxin is found in detergent-insoluble rafts/domains at the cell surface of hippocampal neurons but is internalized via a raft-independent mechanism. J Biol Chem. 2001; 276(12):9182–9188. [PubMed: 11113142]

(51). Popova-Butler A, Dean DH. Proteomic analysis of the mosquito *Aedes aegypti* midgut brush border membrane vesicles. J Insect Physiol. 2009; 55(3):264–272. [PubMed: 19133270]

(52). Pauchet Y, Muck A, Svatos A, Heckel DG. Chromatographic and electrophoretic resolution of proteins and protein complexes from the larval midgut microvilli of *Manduca sexta*. Insect Biochem Mol Biol. 2009; 39(7):467–474. [PubMed: 19464367]

(53). Tchankouo-Nguetcheu S, Khun H, Pincet L, Roux P, Bahut M, Huerre M, Guette C, Choumet V. Differential protein modulation in midguts of *Aedes aegypti* infected with chikungunya and dengue 2 viruses. PLoS One. 2010; 5(10):e13149. [PubMed: 20957153]

(54). Biron DG, Agnew P, Marché L, Renault L, Sidobre C, Michalakis Y. Proteome of *Aedes aegypti* larvae in response to infection by the intracellular parasite *Vavraia culicis*. Int J Parasitol. 2005; 35(13):1385–1397. [PubMed: 16102770]

(55). Foster LJ, de Hoog CL, Mann M. Unbiased quantitative proteomics of lipid rafts reveals high specificity for signaling factors. Proc Natl Acad Sci U S A. 2003; 100(10):5813–5818. [PubMed: 12724530]

(56). Babuke T, Tikkanen R. Dissecting the molecular function of reggie/flotillin proteins. Eur J Cell Biol. 2007; 86(9):525–532. [PubMed: 17482313]

(57). Zhai J, Ström A-L, Kilty R, Venkatakrishnan P, White J, Everson WV, Smart EJ, Zhu H. Proteomic characterization of lipid raft proteins in amyotrophic lateral sclerosis mouse spinal cord. FEBS Journal. 2009; 276(12):3308–3323. [PubMed: 19438725]

(58). Williamson R, Thompson AJ, Abu M, Hye A, Usardi A, Lynham S, Anderton BH, Hanger DP. Isolation of detergent resistant microdomains from cultured neurons: detergent dependent alterations in protein composition. BMC Neurosci. 2010; 11:120. [PubMed: 20858284]

(59). Blonder J, Hale ML, Lucas DA, Schaefer CF, Yu L-R, Conrads TP, Issaq HJ, Stiles BG, Veenstra TD. Proteomic analysis of detergent-resistant membrane rafts. Electrophoresis. 2004; 25(9):1307–1318. [PubMed: 15174053]

(60). Ferreira LM, Romao TP, de-Melo-Neto OP, Silva-Filha MH. The orthologue to the Cpm1/Cqm1 receptor in *Aedes aegypti* is expressed as a midgut GPI-anchored alpha-glucosidase, which does not bind to the insecticidal binary toxin. Insect Biochem Mol Biol. 2010; 40(8):604–610. [PubMed: 20685335]

(61). Seron TJ, Hill J, Linser PJ. A GPI-linked carbonic anhydrase expressed in the larval mosquito midgut. J Exp Biol. 2004; 207(Pt 26):4559–4572. [PubMed: 15579552]

(62). Strigini M, Cantera R, Morin X, Bastiani MJ, Bate M, Karagogeos D. The IgLON protein Lachesin is required for the blood-brain barrier in *Drosophila*. Mol Cell Neurosci. 2006; 32(1–2): 91–101. [PubMed: 16682215]

(63). Salaun C, Greaves J, Chamberlain LH. The intracellular dynamic of protein palmitoylation. J Cell Biol. 2010; 191(7):1229–1238. [PubMed: 21187327]

(64). Yang W, Di Vizio D, Kirchner M, Steen H, Freeman MR. Proteome scale characterization of human S-acylated proteins in lipid raft-enriched and non-raft membranes. Molecular & cellular proteomics : MCP. 2010; 9(1):54–70.

(65). Ren J, Wen L, Gao X, Jin C, Xue Y, Yao X. CSS-Palm 2.0: an updated software for palmitoylation sites prediction. Protein Eng, Des Sel. 2008; 21(11):639–644. [PubMed: 18753194]

(66). Garczynski SF, Adang MJ. *Bacillus thuringiensis* CryIA(c) δ-endotoxin binding aminopeptidase in the *Manduca sexta* midgut has a glycosyl-phosphatidylinositol anchor. Insect BiochemMolBiol. 1995; 25:409–415.

(67). Zhang N, Shaw ARE, Li N, Chen R, Mak A, Hu X, Young N, Wishart D, Li L. Liquid chromatography electrospray ionization and matrix-assisted laser desorption ionization tandem mass spectrometry for the analysis of lipid raft proteome of monocytes. Anal Chim Acta. 2008; 627(1):82–90. [PubMed: 18790130]

(68). Mannova P, Fang R, Wang H, Deng B, McIntosh MW, Hanash SM, Beretta L. Modification of host lipid raft proteome upon hepatitis C virus replication. Molecular & cellular proteomics : MCP. 2006; 5(12):2319–2325.

(69). Wilfong RF, Neville DM. The isolation of a brush border membrane fraction from rat kidney. J Biol Chem. 1970; 245(22):6106–6112. [PubMed: 4320796]

(70). Donowitz M, Singh S, Salahuddin FF, Hogema BM, Chen Y, Gucek M, Cole RN, Ham A, Zachos NC, Kovbasnjuk O, Lapierre LA, Broere N, Goldenring J, deJonge H, Li X. Proteome of murine jejunal brush border membrane vesicles. J Proteome Res. 2007; 6(10):4068–4079. [PubMed: 17845021]

(71). Zheng YZ, Berg KB, Foster LJ. Mitochondria do not contain lipid rafts, and lipid rafts do not contain mitochondrial proteins. J Lipid Res. 2009; 50(5):988–998. [PubMed: 19136664]

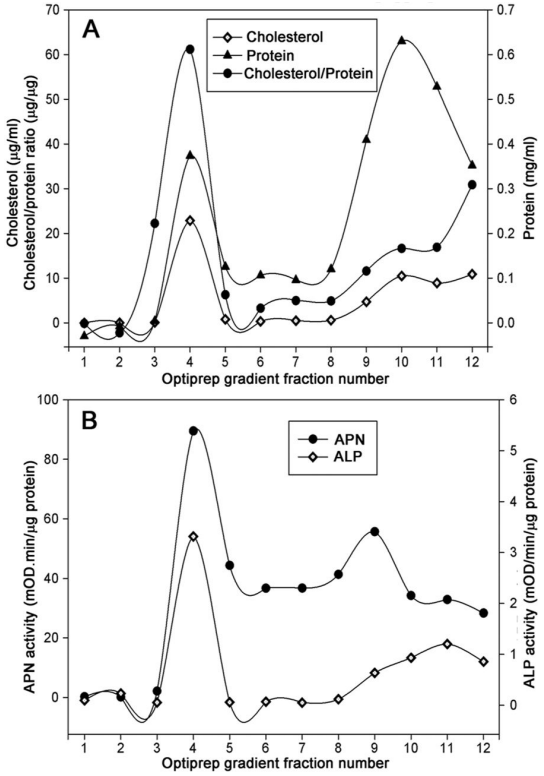

Figure 1.

Distribution of cholesterol and total protein content (A), aminopeptidase and alkaline phosphatase activity (B) across the Optiprep gradient fractions. Whole body BBMV was prepared and extracted with 1%Triton X-100 on ice with MBCD, and the membranes were floated in an Optiprep multistep gradient solution. After Optiprep step gradient ultracentrifugation the gradient was fractionated from the top to the bottom. The cholesterol and total protein content, APN and ALP activity of different Optiprep gradient fractions were determined as indicated in Materials and Methods. Fractionation of the gradient (12 × 1 mL) resulted in detection of a small protein peak observed within the 5–30% Optiprep zone (buoyant fractions 4–5), whereas the bulk of proteins were retained at the bottom of the gradient. Cholesterol was enriched in detergent insoluble and low density Optiprep gradient fraction.

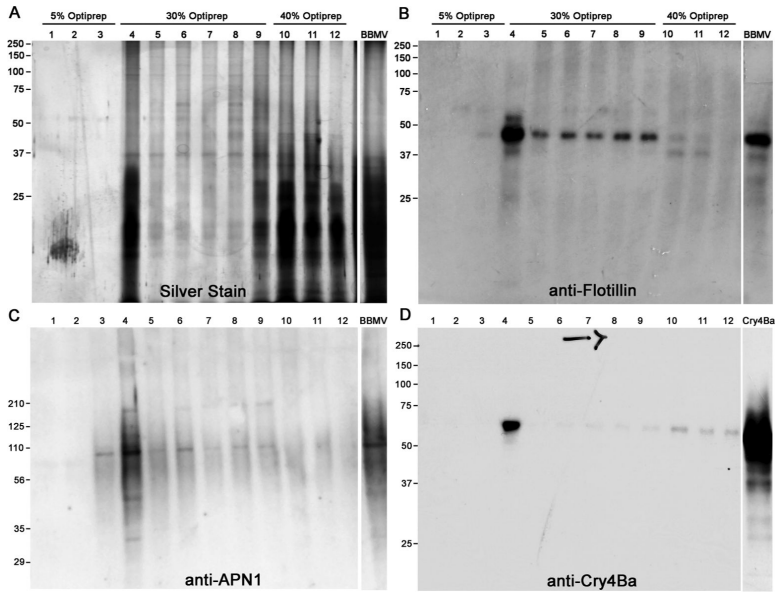

Figure 2.

Distribution of proteins and lipid raft marker proteins across the Optiprep gradient fractions analyzed by immunoblotting. Lipid raft were isolated from whole body BBMV as described in Materials and Methods. An equal volume of each gradient fraction was analyzed by 10% SDS-PAGE followed by silver staining (A), and immunoblotting with anti-Flotillin-1 (B), anti-AgAPN1, (C) and anti- Cry4Ba (D) antisera.

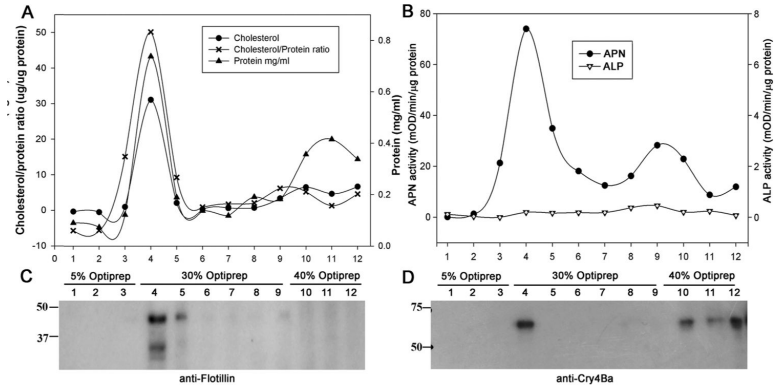

Figure 3.

Effect of MBCD on Protein, Cholesterol, Cry4Ba toxin, APN and ALP distribution in *Aedes* lipid raft fractions. Isolation of lipid rafts from *A. aegypti* BBMV with pre incubation of MBCD followed by detergent solubilization. Triton X-100 insoluble complexes were prepared (see Materials and Methods) centrifuged through a 5%:30%:40% Optiprep step gradient and 1-ml fractions assayed for Cholesterol and total protein content (A), APN & ALP enzyme activity (B), Flot-1 immunoblot (C) and Cry4Ba toxin blot (D). Treatment of BBMV with 20 mM MBCD had no effect on the cholesterol and protein content of lipid raft fractions.

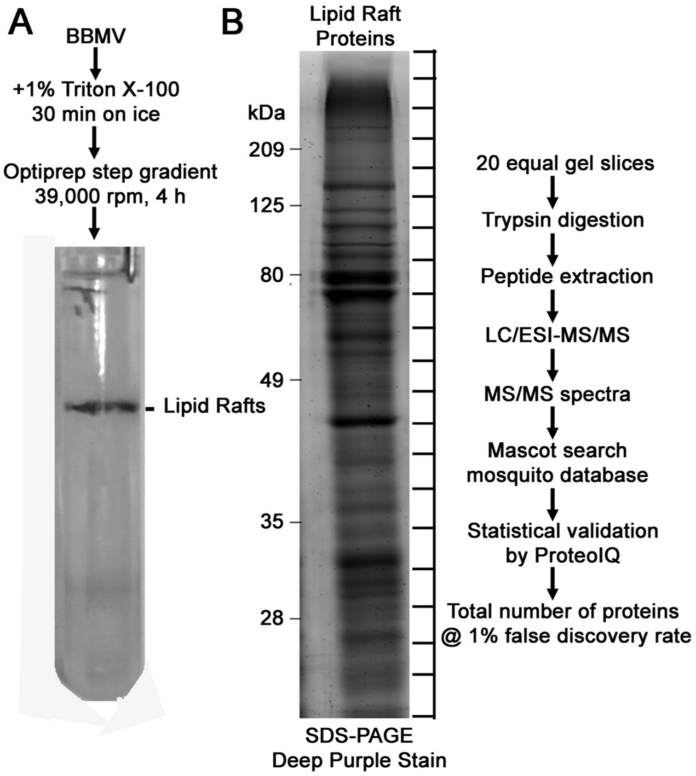

Figure 4.

Schematic representation of *Aedes* lipid rafts isolation and mass spectrometry analysis procedures. Lipid rafts were prepared from the BBMV as described in Materials and Methods. A representative centrifuge tube picture of the gradient with opalescent lipid rafts band obtained after centrifugation is shown (A). Detergent insoluble proteins (15 μg) were resolved on 10% SDS-PAGE and stained with Deep Purple™ total protein stain. Gel bands were sliced equally and digested with trypsin. The resulting peptides were analyzed by LC-MS/MS (B).

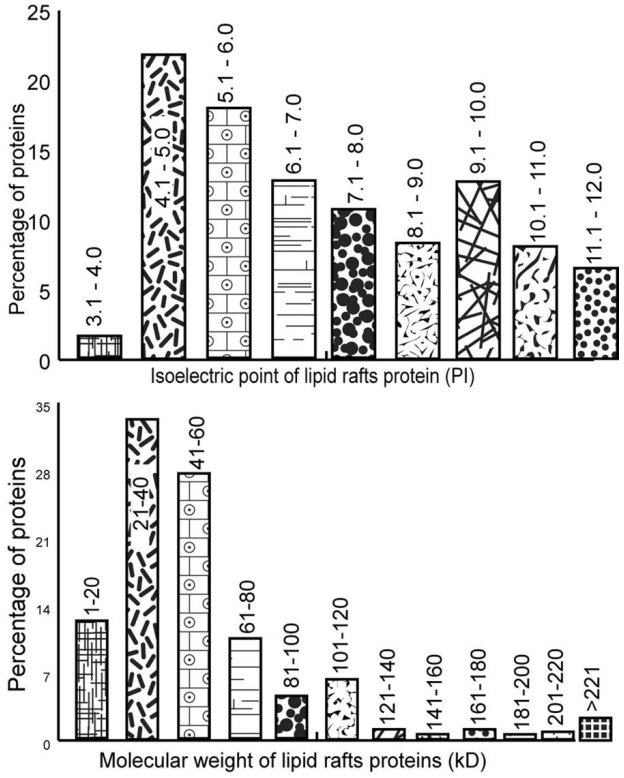

Figure 5.

*In **silico*** analysis of pI and kD values for lipid rafts proteins. According to their primary database sequences pI values were calculated using the ProtParam tool on the ExPASy server (A) and molecular mass values (in kDa) were calculated using the ProteoIQ tool (B).

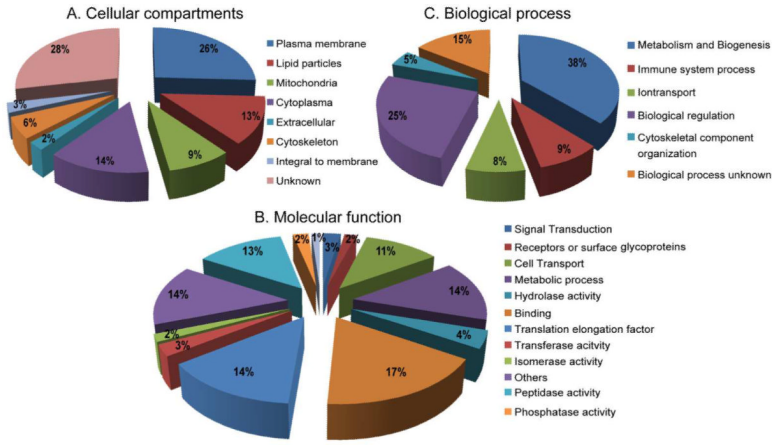

Figure 6.

Classification of identified *Aedes* lipid rafts proteins based on GO for cellular component (A), molecular function (B), and biological process (C). Numbers in percentages (%) correspond to the numbers of GO terms assigned for particular GO category.

Table 1

GPI anchor prediction for proteins in the *A. aegypti* lipid raft fraction. Results for the GPI-anchor prediction from SignalP 3.0 which predicts N-terminal secretory signal and Big PI, GPI SOM, FragAnchor and PredGPI which predicts C-termiral GPI anchor-specific signal. GPI Anchored is the composite of C- and N-termination signal predictions plus Signal P.

	VectorBase acc. no.	Protein Name	Signal Peptide	NN Score	BigPI	Score	Frag Anchor	Score	PredGPI	Score	GPI Anchored
R2	AAEL000904	Acetylcholinesterase	●	0.991	●	3.83E-04	●	0.999952	●	Probable	●
R_1 & R_2	AAEL005821	Alanyl aminopeptidase	●	0.999	●	3.86E-04	●	0.999889	●	Highly probable	●
R_1 & R_2	AAEL005808	Alanyl aminopeptidase	●	1	●	4.77E-04	●	0.999982	●	Highly probable	●
R_1 & R_2	AAEL003313	Alkaline phosphatase	●	0.998	●	7.03E-04	●	0.999894	●	Highly probable	●
R_1 & R_2	AAEL003309	Alkaline phosphatase	●	1	●	7.62E-04	●	0.999979	●	Highly probable	●
R_1 & R_2	AAEL003298	Alkaline phosphatase	●	0.999	○	5.70E-01	○	0.030191	○	Not GPI-anchored	○
R_1 & R_2	AAEL003286	Alkaline phosphatase	●	0.992	○	6.61E-01	○	0.002292	○	Not GPI-anchored	○
R1	AGAP011302	Alkaline phosphatase	○	0.107	○	7.30E-01	○	0.041705	○	Not GPI-anchored	○
R_1 & R_2	AAEL011176	Alkaline phosphatase	●	0.96	○	9.45E-01	○	0.000028	○	Not GPI-anchored	○
R_1 & R_2	AAEL010532	Alpha-amylase	●	1	●	2.32E-04	●	0.99999	●	Highly probable	●
R_1 & R_2	AAEL010540	Alpha-amylase	●	0.998	○	3.85E-03	●	0.99999	●	Highly probable	●
R_1 & R_2	AAEL010537	Alpha-amylase	●	0.997	●	1.51E-03	●	0.999985	●	Highly probable	●
R1	CPIJ013171	Alpha-amylase	●	1	●	9.58E-04	●	0.999988	●	Highly probable	●
R_1 & R_2	AAEL014710	Alpha-amylase	●	0.995	●	4.38E-04	●	0.999997	●	Probable	●
R1	AAEL009569	Apolipoprotein D	●	0.998	●	4.37E-04	●	0.999974	●	Highly probable	●
R_1 & R_2	AAEL010986	Apyrase	○	0.016	●	2.41E-03	●	0.999992	●	Probable	○
R1	CPIJ008529	Beta-glucosidase	○	0.008	○	2.58E-02	●	0.992575	●	Probable	○
R_1 & R_2	AAEL009323	Carbonic anhydrase	●	0.991	●	3.81E-04	●	0.999965	●	Highly probable	●
R1	AAEL006383	Chymotrypsin, putative	●	0.997	●	2.35E-04	●	0.999993	●	Highly probable	●
R2	AAEL015105	Chymotrypsin	●	0.997	●	3.01E-04	●	0.999991	●	Highly probable	●
R_1 & R_2	AAEL011551	Conserved hypothetical protein	●	0.999	●	5.23E-04	●	0.999995	●	Highly probable	●
R_1 & R_2	AAEL004873	Conserved hypothetical protein	●	1	●	4.13E-04	●	0.999891	●	Highly probable	●
R_1 & R_2	AAEL008801	Conserved hypothetical protein	○	0	○	7.61E-02	●	0.999433	○	Not GPI-anchored	○
R_1 & R_2	AAEL008478	Conserved hypothetical protein	●	0.994	○	8.83E-03	○	Pot. false +	●	Highly probable	●
R_1 & R_2	AAEL010520	Conserved hypothetical protein	●	0.998	○	7.33E-01	●	0.99997	●	Probable	○

	VectorBase acc. no.	Protein Name	Signal Peptide	NN Score	BigPI	Score	Frag Anchor	Score	PredGPI	Score	GPI Anchored
R_1 & R_2	AAEL010266	Conserved hypothetical protein	○	0	○	1.31E-02	○	Pot. false +	●	Weakly probable	○
R_1 & R_2	AAEL008857	Deoxyribonuclease I	○	0.001	●	2.61E-03	●	0.999143	●	Probable	○
R2	AAEL009316	Dipeptidyl carboxypeptidase	○	0	○	6.15E-03	●	0.999956	●	Probable	
R_1 & R_2	AAEL007201	Glutamyl aminopeptidase	●	0.525	○	2.75E-01	●	0.23483	●	Weakly probable	○
R_1 & R_2	AAEL009237	Glycoside hydrolases	●	1	○	6.07E-03	●	0.999973	●	Highly probable	○
R_1 & R_2	AAEL015573	Glycoside hydrolases	○	0.019	●	6.21E-02	●	0.949126	●	Highly probable	○
R_1 & R_2	AAEL015020	Glycoside hydrolases	●	1	●	6.07E-03	●	0.99997	○	Highly probable	○
R_1 & R_2	AAEL009295	Lachesin	●	0.995	●	3.64E-04	●	0.999928	●	Highly probable	●
R_1 & R_2	AAEL015070	Membrane-bound alkaline phosphatase	●	0.867	●	7.54E-04	●	0.999946	●	Probable	●
R1	AAEL014842	Multiple inositol polyphosphate phosphatase	●	0.998	●	5.18E-03	●	0.999507	●	Weakly probable	●
R2	AAEL015040	Multiple inositol polyphosphate phosphatase	●	0.996	○	7.20E-03	●	0.999329	●	Weakly probable	●
R_1 & R_2	AAEL006371	Oviductin	○	0	○	2.98E-01	●	0.999646	○	Not GPI-anchored	○
R_1 & R_2	AAEL008702	Prolylcarboxypeptidase	●	0.999	○	2.89E-01	○	n/a	○	Not GPI-anchored	●
R_1 & R_2	AAEL012778	Protease m1 zinc metalloprotease	●	0.98	●	4.13E-04	●	0.999991	●	Highly probable	●
R_1 & R_2	AAEL008155	Protease m1 zinc metalloprotease	●	0.994	○	2.78E-01	○	0.103862		Not GPI-anchored	●
R_1 & R_2	AAEL012776	Protease m1 zinc metalloprotease	●	1	○	5.11E-01	○	0.005453	●	Weakly probable	○
R_1 & R_2	AAEL012774	Protease m1 zinc metalloprotease	●	0.993	○	7.47E-01	○	0.000355	○	Not GPI-anchored	○
R_1 & R_2	AAEL012783	Protease m1 zinc metalloprotease	●	0.998	●	1.07E-03	●	0.999982	●	Highly probable	●
R_1 & R_2	AAEL008163	Protease m1 zinc metalloprotease	●	1	○	7.16E-01	○	0.000179	○	Not GPI-anchored	○
R_1 & R_2	AAEL012786	Protease m1 zinc metalloprotease	●	0.989	○	2.30E-01	○	0.000943	○	Not GPI-anchored	○
R_1 & R_2	AAEL013899	Protease m1 zinc metalloprotease	○	0	○	4.70E-01	○	0.000441	○	Not GPI-anchored	○
R_1 & R_2	AAEL008162	Protease m1 zinc metalloprotease	●	1	○	2.33E-01	○	0.013946	○	Not GPI-anchored	○
R_1 & R_2	AAEL012779	Protease m1 zinc metalloprotease	○	0	○	9.77E-04	●	0.999955	●	Probable	○
R_1 & R_2	AAEL000859	Putative uncharacterized protein	●	0.997	○	3.98E-03	●	0.999989	●	Highly probable	●
R1	AAEL006271	Superoxide dismutase (Cu-Zn)	●	1	●	8.65E-04	●	0.999962	●	Weakly probable	●
R_1 & R_2	AAEL008607	Tep3	○	0	○	4.88E-03	●	0.999985	●	Weakly probable	○
R_1 & R_2	AAEL011641	Transferrin	●	0.993	●	5.69E-02	○	Pot. false +	●	Weakly probable	●
R_1 & R_2	AAEL013320	Translocon-associated protein, delta subunit	●	1	○	2.24E-01	○	n/a	●	Probable	●

	VectorBase acc. no.	Protein Name	Signal Peptide	NN Score	BigPI	Score	Frag Anchor	Score	PredGPI	Score	GPI Anchored
R_1 & R_2	AAEL005614	Trypsin	●	1	○	2.09E-01	○	Pot. false +	○	Not GPI-anchored	●
R1	AAEL008079	Trypsin-alpha	●	0.974	●	4.27E-04	●	1	●	Highly probable	●
R_1 & R_2	AAEL008097	Trypsin-Beta	●	0.987	○	1.16E-02	○	Pot. false +	●	Weakly probable	●
R1	AAEL005269	Ubiquinol-cytochrome c reductase complex core protein	●	0.914	●	1.67E-02	○	n/a	●	Weakly probable	●
R_1 & R_2	AAEL007777	Vacuolar ATP synthase subunit S1	●	1	●	6.61E-01	○	n/a	●	Weakly probable	○
R_1 & R_2	AAEL006023	Vanin-like protein 1	●	0.842	●	2.83E-03	●	0.999998	○	Not GPI-anchored	●
R2	AAEL006034	Vanin-like protein	●	0.928	●	1.17E-03	●	0.999967	●	Highly probable	●
R_1 & R_2	AAEL001840	Zinc carboxypeptidase	●	0.994	○	4.84E-01	○	0.018004	○	Not GPI-anchored	○
R_1 & R_2	AAEL008600	Zinc carboxypeptidase	●	0.996	○	4.90E-01	○	0.000595	○	Not GPI-anchored	○
R_1 & R_2	AAEL008609	Zinc carboxypeptidase	○	0.002	○	1.17E-01	○	0.177718	○	Not GPI-anchored	○
R_1 & R_2	AAEL001844	Zinc carboxypeptidase	●	1	○	2.67E-01	○	0.000055	○	Not GPI-anchored	○

Symbol `●' denoting a positive prediction while '○' indicates a negative prediction.

Note: `$R_1$' indicates protein present in only first biological replicate, `R_2' indicates protein present in only second biological replicate and `R_1 & R_2' indicates protein present in both biological replicates.

Table 2

Alkaline phosphatases and Aminopeptidases with Cry Receptor Function Identified in DRMs*.

Replicate	VectorBase Ace. No.	Mascot Score	Protein	Interacting toxin/s	Reference
R_1 & R_2	AAEL003286 (ALP3)	329	Alkaline phosphatase	Cry11Ba	(16) Likitvivatanavong et al. (2011)
R_1 & R_2	AAEL003298 (ALP3)	592	Alkaline phosphatase	Cry4Ba	(28) Bayareddy et al. (2009)
R_1 & R_2	AAEL003313 (ALP5)	829	Alkaline phosphatase	Cry4Ba	(28) Bayareddy et al. (2009)
R_1 & R_2	AAEL015070 (ALP7)	235	Alkaline phosphatase	Cry4Ba	(28) Bayareddy et al. (2009), (19) Dechklar et. al. (2011)
R_1 & R_2	AAEL012778 (APN1)	2564	Aminopeptidase	Cry4Ba, Cry11Aa, Cry11Ba	(21) Chen et al (2009); (16) Likitvivatanavong et al. (2011), (22)
R_1 & R_2	AAEL008155 (APN2)	2435	Aminopeptidase	Cry11Aa	(21) Chen et al. (2009)
R_1 & R_2	AAEL012776 (APN4)	673	Aminopeptidase	Cry4Ba	(28) Bayareddy et al. (2009)
R_1 & R_2	AAEL012774 (APN4)	651.51	Aminopeptidase	Cry11	(21) Chen et al. (2009)

Note: `R_1 & R_2' (highlight in yellow) indicates protein present in both biological replicates.

*Cry11Aa and Cry11Ba receptor ALP1 (AAEL009077) identified by (18) Fernandez et al. (2006) and (16) Likitvivatanavong et al. (2011) was not identified in DRMs.